I. RAMAN SPECTRA OF SOME SILICON COMPOUNDS

II. KINETICS OF OXIDIZED SILVER SOLUTIONS

Thesis by

Fred B. Stitt

In Partial Fulfillment of the

Requirements for the Degree of Doctor of Philosophy

California Institute of Technology

Pasadena, California

1936

Propositions Submitted for Defense on April 16, 1936.

1) BCl_3 has a planar structure. In general, compounds or radicals of type AB_3 are planar if resonance with double bond structures is possible; otherwise they are pyramidal.

2) Two of the fundamental vibration frequencies of silane suggested by Steward and Nielsen (Phy. Rev. 47, 828, 1935) are probably incorrect.

3) The spontaneous transformation of ammonium cyanate into urea in solution involves reaction between ammonium and cyanate ions. The activation probably occurs in the cyanate ion.

4) In the measurement of the polarization of Raman lines, the simultaneous use of a plate calibration device at the slit followed by a Wollaston prism within the collimator tube of the spectrograph has advantages over other methods that have been used.

5) The rate of reduction of nitric acid solutions of argentic silver may reasonably be explained by assuming that the following reactions occur simultaneously:

$$2\ AgO^+ = 2Ag^+ + O_2$$

$$AgO^+ + H_2O = Ag^+ + H_2O_2$$

6) In cases of accidental degeneracy due to resonance, the total intensity of Raman lines or of infra-red bands should be the same as if accidental degeneracy were not present.

7) The apparent temperature change of dipole moment of NO_2 may be explained by King's hypothesis of the existence of two types of NO_2 molecules.

8) The static forces present in the equilibrium configuration of a molecule cannot be evaluated from an infinitesimal vibrational analysis alone.

Respectfully submitted,

Fred B. Stitt

Fred B. Stitt

Abstract

I. Raman Spectra of Some Silicon Compounds.

SiH_4: Two lines were observed in the gas and liquid. With the help of infra-red data a complete assignmentis made for the vibrational spectrum of silane.

$Si_2H_6(g)$ and $Si_2Cl_6(l)$: Three lines were observed in $Si_2H_6(g)$ and some fourteen in $Si_2Cl_6(l)$. Polarization measurements on the stronger lines of Si_2Cl_6 were made by a convenient method which is described.

From a consideration of the relations among the modes of vibration of similar molecules having different symmetry, the analysis of the observed lines is facilitated by a knowledge of the assignments of the fundamental frequencies of SiH_4, $HSiCl_3$, and $BrSiCl_3$. A definite assignment is made for the three observed lines of Si_2H_6. A tentative assignment of the observed lines of Si_2Cl_6 is made and some evidence is presented for the existence of internal rotation in this molecule at room temperature.

II. Kinetics of Oxidized Silver Solutions.

The behavior of a number of reducing agents toward nitric acid solutions of argentic silver and of ozone has been observed. Argentic solutions may be reduced quantitatively by titration with any of a number of reducing agents using the disappearance of the argentic color as end point.

The rate of oxidation by ozone of nitric acid solutions of silver nitrate and the rate of decomposition of these oxidized solutions has been studied using suitable technique and method of analysis. The reduction rate is found to fit the differential equation

$$-\frac{d(Ag^{++})}{dt} = k_2 \frac{(Ag^{++})^2}{(Ag^{+})} + k_4 \frac{(Ag^{++})^4}{(Ag^{+})} \qquad (4)$$

indicating simultaneous occurrence of two slow reactions. (The oxidized silver is assumed to be principally in the divalent state.)

The oxidation rate is found to fit the equation

$$\frac{d(Ag^{++})}{dt} = k_o (Ag^{+})(O_3) - \text{reduction rate} \qquad (10)$$

The steady state reached on prolonged oxidation by ozone of nitric acid solutions of silver nitrate is shown to correspond approximately to the point where $d(Ag^{++})/dt = 0$ in equation 10 with the reduction rate given by equation 4.

Equilibrium between three valence states of silver is postulated, probably according to the equation

$$AgO^{+} + Ag^{+} + 2\,H^{+} = 2\,Ag^{++} + H_2O. \qquad (2)$$

The oxidation mechanism is probably

$$AgO^{+} + H_2O = Ag^{+} + H_2O_2$$

combined with equation 2.

The fourth order reduction reaction may be

$$H_2O + 2\,Ag^{++} + AgO^{+} = 3\,Ag^{+} + O_2 + 2\,H^{+}.$$

Table of Contents

THE RAMAN SPECTRA OF SOME SILICON COMPOUNDS

INTRODUCTION

The study of the Raman spectrum of a compound constitutes perhaps the simplest experimental method of finding fundamental vibrational frequencies of a molecule. Unfortunately the Raman spectrum alone does not usually reveal all of these frequencies. For complete knowledge of these a study of the infra-red absorption spectrum is usually also necessary, and frequently additional information such as accurate specific heat data is needed as well.

These vibrational frequencies are essential for the calculation of thermodynamic quantities of a substance from a knowledge of the energy levels of its molecules. They are also frequently useful in determining molecular structure.

In this work we have studied the Raman spectra of silane (SiH_4), disilane (Si_2H_6), and disilicon hexachloride (Si_2Cl_6) a) to determine for thermodynamic calculations as many of the fundamental vibrational frequencies as possible, and b) to decide so far as is possible from the data whether or not free rotation of the two $-SiCl_3$ radicals of Si_2Cl_6 with respect to each other occurs under ordinary conditions.

Reprinted from THE JOURNAL OF CHEMICAL PHYSICS, Vol. 4, No. 1, 82, January, 1936
Printed in U. S. A.

The Raman Spectrum and Fundamental Vibration Frequencies of Silane (SiH_4)

We have found the Raman lines for silane, SiH_4, shown in Table I.

Two extremely faint lines were observed at 1195 ± 20 cm^{-1} and 1825 ± 20 cm^{-1}, but their presence is doubtful and they cannot safely be ascribed to SiH_4.

When the gas was exposed to the mercury arc in quartz, a slow decomposition occurred with the deposition of a yellow-white solid. This presumably consists of unsaturated polymerized hydrides. The lines from the gas were obtained without difficulty with Hg 3650, 4078 and 4358A as the exciting radiation.

The silane was prepared by the method of Stock.[1] The final product was purified by repeated fractionation and probably contained less than 0.1 percent impurity. It is of interest to note that our magnesium silicides, prepared by Stock's method, did not yield appreciable quantities of silicon hydrides when treated with NH_4Br in NH_3 (l). This procedure has been found satisfactory by Johnson and Isenberg[2] when the silicide is prepared by a different method.

Silane doubtless has a regular tetrahedral structure. Calling the completely symmetrical vibrational frequency ν_1, the symmetrical twofold degenerate frequency ν_2, and the high and low threefold degenerate frequencies ν_3 and ν_4, respectively, the selection rules[3] permit all four frequencies in the Raman effect, and only ν_3 and ν_4 in the infrared. Steward and Nielsen[4] have measured the infrared absorption bands of silane. The combined infrared and Raman data have led us to the following assignments of the fundamentals: $\nu_1 = 2187$ cm^{-1}, $\nu_2 = 978$ cm^{-1}, $\nu_3 = 2183$ cm^{-1}, $\nu_4 = 910$ cm^{-1}. The strong sharp Raman line 2187 is taken as ν_1. This choice is based on a characteristic of tetrahedral molecules XY_4,[5] namely, that the completely symmetric vibration appears sharp and most intense in the Raman effect.

$\nu_3 = 2183$ cm^{-1}, and ν_4 in the neighborhood of 910 to 980 cm^{-1}, must also be the correct assignments of the two strongest infrared bands. Steward and Nielsen chose $\nu_4 = 910$ cm^{-1}. The infrared band in that region[4] is very complex, and it is possible that the band center is not where they have chosen it. Judging from the appearance of the band the center is not as high as 978 cm^{-1}. Accordingly, with Steward and Nielsen, we have taken $\nu_4 = 910$ cm^{-1}, and have considered the Raman line at 978 cm^{-1} to be ν_2. However, there is the possible alternative that $\nu_4 = 978$ cm^{-1} and that ν_2 is yet to be found, although the above assignment seems more likely, with perhaps some uncertainty as to the numerical value for ν_4. Using the valence-force formulae (Eq. (36)) of Miss Rosenthal[6] which fits the frequencies of methane, CH_4[7] ($\nu_1 = 2915$ cm^{-1}, $\nu_2 = 1530$ cm^{-1}, $\nu_3 = 3020$ cm^{-1}, $\nu_4 = 1320$ cm^{-1}) with an error of about three percent, one calculates $\nu_2 \leqq 1042$ cm^{-1} if $\nu_4 = 910$ cm^{-1} or $\nu_2 \leqq 1121$ cm^{-1} if $\nu_4 = 978$ cm^{-1}.

TABLE I. *The Raman spectrum of silane.*

	$\Delta\nu$ cm^{-1}	
$SiH_4(g)$, at 5 atmos.	2187	Strong, sharp
	978 $\pm$5	Very faint
$SiH_4(l)$, at -120°C	2175	Very strong, sharp
	967 $\pm$10	Medium, diffuse

TABLE II. *Vibrational spectrum of silane.*

	OBSERVED (cm^{-1})	INTENSITY	CALCULATED (cm^{-1})
ν_4	910	50	(910)
ν_2	978	Raman, medium	(978)
$\nu_3 - \nu_4$ or $\nu_1 - \nu_4$	1260	0.1	1273 or 1277
$\nu_2 + \nu_4$	1900	0.1	1888
ν_3	2183	20	(2183)
ν_1	2187	Raman, strong	(2187)
$\nu_1 + \nu_4$ or $\nu_3 + \nu_4$	3095	1.0	3093, 3097
$\nu_2 + \nu_3$	3153	1.0	3161
$2\nu_3$	4360	0.1	4366
?	1680	—	—

The complete assignment (compare reference 4) chosen for the vibrational spectrum of SiH_4 is shown in Table II.

The assignments here given to 3153 cm^{-1} and 1901 cm^{-1} differ from Steward and Nielsen's, but are justified by the appearance, with appreciable intensity, of the analogous bands in the methane spectrum.[7]

FRED B. STITT
DON M. YOST

Gates Chemical Laboratory,
Pasadena, California,
December 5, 1935.

[1] Stock and Somieski, Ber. **49**, 111 (1916).
[2] Johnson and Isenberg, J. Am. Chem. Soc. **57**, 1349 (1935).
[3] E. Bright Wilson, Jr., J. Chem. Phys. **2**, 432 (1934); G. Placzek, *Rayleigh Streuung und Raman Effekt* (Leipzig, 1934).
[4] Steward and Nielsen, Phys. Rev. **47**, 828 (1935).
[5] See for example data in Kohlrausch, *Der Smekal-Raman-Effekt* (Berlin, 1931); also Placzek, reference 3.
[6] Rosenthal, Phys. Rev. **46**, 730 (1934).
[7] Vedder and Necke, Zeits. f. Physik **86**, 137 (1933).

FEBRUARY, 1937 JOURNAL OF CHEMICAL PHYSICS VOLUME 5
Printed in U. S. A.

The Analysis of the Raman Spectra of $Si_2Cl_6(l)$ and of $Si_2H_6(g)$*

FRED STITT AND DON M. YOST
California Institute of Technology, Pasadena, California

(Received October 31, 1936)

The Raman spectra of $Si_2H_6(g)$ and of $Si_2Cl_6(l)$ have been photographed. Polarization measurements of the stronger lines of Si_2Cl_6 have been made. From a consideration of the relations among the modes of vibration of similar molecules having different symmetry, the analysis of the observed lines is facilitated by a knowledge of the assignments of the fundamental frequencies of SiH_4, $HSiCl_3$ and $BrSiCl_3$. A definite assignment is made for the three observed lines of Si_2H_6. A tentative assignment of the observed lines of Si_2Cl_6 is made and some evidence is presented for the existence of internal rotation in this molecule at room temperature.

IN addition to determining and assigning some of the fundamental vibration frequencies of disilane and of disilicon hexachloride, we have attempted in this investigation to determine whether or not internal rotation is present in the Si_2Cl_6 molecule at room temperature.

EXPERIMENTAL

The disilane used was obtained from Professor Johnson of the University of Chicago, and we wish to express our gratitude to him for his kindness in making the material available to us. It was quite pure, showing, according to Professor Johnson, a molecular weight of 62.6; the formula weight is 62.2.

The disilicon hexachloride was prepared by treating ferrosilicon[1] with chlorine and fractionally distilling the product four or five times. It boiled at 145°±0.5°.

The spectrum of gaseous disilane was photographed with radiation from a mercury arc. A Pyrex Raman tube was used to avoid possible decomposition since Hg 2537A was found to decompose SiH_4.[2] When the Si_2Cl_6 was photographed in a Pyrex tube without a filter it showed some decomposition with the appearance of small brown flakes of silicon. An acid quinine chloride solution as filter absorbed almost completely all lines of the mercury arc of higher frequency than the Hg 4358 group, and no decomposition occurred. As Raman lines excited by the 4047 group were observed in the absence of the filter, the decomposition was probably due to the Hg 3650 group.

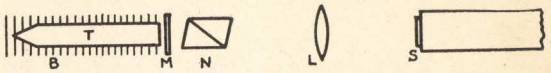

FIG. 1. Experimental arrangement for polarization measurements. *M*, half-wave mica plate; *N*, Nicol prism; *S*, step weakener on slit of spectrograph; *T*, Raman tube; *L*, condensing lens; *B*, parallel black screens.

Polarization measurements were made on the stronger lines of Si_2Cl_6 (*l*). The experimental arrangement used for these measurements is shown in Fig. 1. This arrangement suffers the disadvantage that a separate exposure must be made for the parallel and perpendicular components,[3] but possesses the two following important advantages: (1) The use of a step weakener on the slit[4] automatically calibrates the photographic plate, the blackening along the length of each spectral line varying in steps of known relative intensity of illumination. Thus both the source and the exposure time for calibration are the same as for the image, an important factor where low intensities and long exposure times are involved. (2) The use of a half-wave mica plate[5] preceding

* Contribution from the Gates and Crellin Laboratories of Chemistry of the California Institute of Technology, No. 574.

[1] Quig and Wilkinson, J. Am. Chem. Soc. **48**, 902 (1926); Martin, J. Chem. Soc. **105**, 2836 (1914).

[2] Stitt and Yost, J. Chem. Phys. **4**, 82 (1936).

[3] An arrangement eliminating this disadvantage is obtained if, in Fig. 1, *M* and *N* be removed and a large aperture Wollaston prism be introduced into the collimator tube of the spectrograph. Correction for polarization due to the spectrograph may then be eliminated by rotating the Wollaston 45° about the axis of the tube from the position in which the two beams emerging from it are in a vertical plane. The mercury arc is placed so that with the Raman tube it determines a plane at 45° to the vertical. This arrangement was not used because a suitable Wollaston prism was not available.

[4] We are indebted to Professor Houston and Dr. C. M. Lewis for allowing us to use a step weakener made by them. See Phys. Rev. **44**, 903 (1933).

[5] We are indebted to Dr. John Strong for suggesting the use of a half-wave plate.

the Nicol prism eliminates the correction for polarization due to the apparatus, and also allows each component to be photographed passing through the spectrograph with the electric vector in the horizontal plane, thus minimizing the loss due to reflection by the prism faces.

For photographing one component (the ||-component for illumination in a vertical plane) the axis of the Nicol prism is horizontal and the axis of the mica plate parallel to that of the Nicol. The only alteration necessary for photographing the other component is to rotate the half-wave plate through 45°, thus rotating by 90° the electric vector of the light passing through it. Tests showed that a 0.048 mm mica sheet serves as a half-wave plate with practically no error from 4400A to 5000A. Only for high frequency shifts from Hg 4358A as an exciting line need a different thickness plate be used.

The step weakener was calibrated at a number of different wave-lengths. For the calibration a low voltage Mazda lamp, such as used in street lights, served as constant source of illumination, and the small, spiral, vertical filament served as a good point source. The inverse square law of illumination was assumed throughout. Five positions giving relative intensities of 1, 0.8, 0.6, 0.4, 0.2 were used, each with exactly one hour exposure time. By microphotometering these continuous spectra at any wave-length the calibration for that wave-length could be made. Eight steps were used having relative transmission values of 1.00, 0.85, 0.61, 0.45, 0.34, 0.26, 0.19, 0.14 at 4384A.

TABLE I. *Raman spectrum of Si_2H_6 (g). Pressure approximately 2 atmos.*

$\Delta\tilde{\nu}$ IN CM^{-1}	NO. OF EXCITING LINES	DESCRIPTION
2163	6	Strong; sharp.
910 to 955	2	Weak; diffuse.
434.5	3	Medium intensity; sharp; appeared also as an anti-Stokes line.

A Raman tube of rectangular cross section was employed in order to minimize reflection of incident light. Parallel black screens for making the incident light approximately parallel were so spaced that only light within about 15° of the vertical could enter the Raman tube. For $\rho=0.86$ the error in ρ is less than 0.02 for incident light at an angle of 20° with the vertical.[6] Eastman I−O plates were used.

The mercury arc was run at constant voltage and showed little fluctuation in current over long periods of time. A 48-hour exposure of each component was taken, the illumination probably being very nearly the same for both components. However, it should be pointed out that, for this work, it is not necessary that the illumination be precisely the same for the two components for accurate results. For practically all compounds

[6] G. Placzek, "Rayleigh-Streuung und Raman-Effekt," *Handbuch der Radiologie*, Band II, Teil 2 (Leipzig, 1934), p. 244.

TABLE II. *Raman spectrum of Si_2Cl_6 (l). (Anti-Stokes lines not included.)*

ν IN CM^{-1}	$\Delta\tilde{\nu}$ IN CM^{-1}	RELATIVE INTENSITY	POLARIZATION RATIO (ρ)	DESCRIPTION
22806	124	8	0.72±0.02	Double line; diffuse. Not resolved in polarization measurements. 132 cm^{-1} portion seems slightly less diffuse than 124 cm^{-1} portion.
22814	132	5		
22759	179	~0.4		Sharp.
22726	212	4	0.86±0.02	Sharp.
22685	354	<<1	—	Hg 4047 as exciting line.
22641	354	<<1		Hg 4339 as exciting line.
22584	354	10	<0.05	Sharp.
22561	377	1		Double; similar to 124, 132 cm^{-1} doublet. 388 cm^{-1} portion seems slightly more intense and less diffuse than 377 cm^{-1} portion.
22551	387			
22517	421	<<<1		Broad; too broad to be $\Delta\nu=425$ cm^{-1} of $SiCl_4$.
22478	460	<<<1		Very weak; moderately diffuse.
22451	487	<<<1		Very broad. Strongest of <<<1 lines. Too intense to be $\Delta\nu=588$ cm^{-1} from Hg 4339.
22405	590	<<<1		Hg 4347 as exciting line.
22373	565	<<1		Moderately diffuse. Too intense for $\Delta\nu=625$ cm^{-1} from Hg 4347 as exciting line.
22348	590	3	0.88±0.03	Rather diffuse.
22313	625	2	<0.5	Moderately diffuse.
22232	706	<<<1		Very weak; moderately diffuse.

TABLE III. *Relations among the irreducible representations of certain symmetry groups.*

T_d	C_{3v}	C_3	D_3	D_{3h}	C_{3v} or D_3	D_{3d}
A_1 A_2 E	A_1 A_2 E	A $E_{1,2}$	A_1 A_2 E	A_1' A_2''	A_1	A_{1g} A_{2u}
T_1	A_2+E			A_1'' A_2'	A_2	A_{2g} A_{1u}
T_2	A_1+E			E' E''	E	E_g E_u

some Raman lines have $\rho=6/7$ for ordinary incident light. If the exposure is somewhat different for the two components, one may find an accurate correction factor to use with the observed ρ values from the fact that the highest ρ is probably actually 6/7. In the present work, the observed values for two lines were 0.86 within narrow limits thus confirming our assumption that the illumination was the same for the two exposures.

On plotting the microphotometer reading for each step as ordinate against the percentage transmission for that step as abscissa for each component, the depolarization ρ is the ratio of the abscissas for the same ordinate on the two curves. (Correction for background was unnecessary as the background was negligible. Note the background radiation also is reduced in known ratios.) The values of ρ thus found choosing different ordinates agreed quite well.

The experimental results are summarized in Tables I and II.

THEORETICAL

Wigner[7] has shown that the normal coordinates for vibrations of a system of point particles belong to (that is, have the linear transformation properties of) definite irreducible representations (IR) of the point group representing the symmetry of the system. The methods for determining, for a given model, how many vibrational frequencies belong to each of the IR of the appropriate group and for determining the selection rules in the Raman and infrared spectrum are now well known.[8]

[7] *Göttingen Nachrichten* (1930), p. 133.

[8] See reference 6, 7; also E. B. Wilson, Jr., Phys. Rev. **45**, 706 (1934), J. Chem. Phys. **2**, 432 (1934) and references given there.

It is instructive to follow (*a*) how the fundamental frequencies for a model with a given number of atoms are distributed among the IR of the appropriate point group as the symmetry of the model is changed from that of one point group to that of another, and (*b*) and (*c*) how the new modes of vibration introduced when the number of atoms in a model is increased, with and without altering the point group symmetry, distribute themselves among the IR of the appropriate point group. The use of such considerations for correlation and assignment of frequencies is frequently very helpful. We will restrict ourselves here to a discussion of examples related to the interpretation of the spectra of Si_2H_6 and Si_2Cl_6.

For studying the distributions referred to in the preceding paragraph the methods already referred to[8] are employed, supplemented by some further considerations. When the symmetry is lowered to that of a subgroup of the original group, those IR of the original group possessing the same characters with respect to the operations of the subgroup merge to form a single IR of the subgroup. Mulliken[9] has published tables showing some of these relations. When the symmetry is altered so that the new point group is not a subgroup of the original one, a correlation between the two is then obtained by seeing how the IR of each reduce to those of the group possessing all elements of symmetry common to the two. For our present purposes we are interested in these relations for the point groups C_{3v}, D_3, D_{3d}, D_{3h}, and T_d; these are shown in Table III. IR designated by **A** are one dimensional, and frequencies associated with them are nondegenerate; those

TABLE IV. *Irreducible representations to which the fundamental frequencies of certain models belong, and selection rules for Raman and infrared spectra.*

FORMULA	SYMMETRY	FREQUENCIES	RAMAN ACTIVE	INFRARED ACTIVE
XY_3	C_{3v}	$2A_1$, $2E$	$2A_1$, $2E$	$2A_1$, $2E$
XY_4	T_d	A_1, E, $2T_2$	A_1, E, $2T_2$	$2T_2$
XY_3Z	C_{3v}	$3A_1$, $3E$	$3A_1$, $3E$	$3A_1$, $3E$
X_2Y_6	D_{2d}	$3A_{1g}$, A_{1u}, $2A_{2u}$ $3E_g$, $3E_u$	$3A_{1g}$, $3E_g$	$2A_{2u}$, $3E_u$
X_2Y_6	D_{3h}	$3A_1'$, A_1'', $2A_2''$ $3E'$, $3E''$	$3A_1'$, $3E'$, $3E''$	$2A_2''$, $3E'$
X_2Y_6	D_3	$4A_1$, $2A_2$, $6E$	$4A_1$, $6E$	$2A_2$, $6E$

Note: By active is meant only that a frequency is permitted to appear, and not that it necessarily does appear.

[9] Phys. Rev. **43**, 294 (1933).

designated with letters **E** and **T** are two and three dimensional, respectively, and the frequencies associated with them are doubly and triply degenerate.

In Table IV are shown the distribution of the fundamental vibrations for several models among the IR of the appropriate point group, and also the selection rules for the fundamentals in their infrared and Raman spectra. For those vibrations belonging to the completely symmetric IR ($\mathbf{A}_1$ of $\mathbf{D}_3$, $\mathbf{A}_1$ of $\mathbf{C}_{3v}$ and of $\mathbf{T}_d$, $\mathbf{A}_1'$ of $\mathbf{D}_{3h}$, and $\mathbf{A}_{1g}$ of $\mathbf{D}_{3d}$) the corresponding Raman lines have a polarization ratio $\rho<6/7$; for all others $\rho=6/7$.

In Table V are shown the Raman selection rules for first overtones and one-one combinations for these same models.

Coordinates belonging to appropriate IR for a given model of X_2Y_6 may be constructed readily from similar coordinates for the XY_3 model. (The normal coordinate for a given vibration is a linear combination of those symmetry coordinates belonging to the IR with which that vibration is associated.) The method is as follows: For each symmetry coordinate of XY_3 construct two for X_2Y_6. In both of these each $-XY_3$ radical vibrates with the XY_3 symmetry coordinate, but in one the two radicals vibrate in phase, in the other 180° out of phase. This will be made clear by reference to Fig. 2, in which are shown the symmetry coordinates thus[10] found from the symmetry coordinates formulated by Howard and Wilson[11] for XY_3. The "in phase" coordinates (those with subscript s) are unchanged by rotation about a twofold axis of the X_2Y_6 model,

TABLE V. *Raman selection rules for first overtones and for one-one combinations of fundamental frequencies of X_2Y_6 models. All are allowed except those shown.*

SYMMETRY	FORBIDDEN RAMAN LINES
$\mathbf{D}_3$	$\mathbf{A}_1+\mathbf{A}_2$
$\mathbf{D}_{3d}$	$(\mathbf{A}_{1g}$ or $\mathbf{A}_{1u})+(\mathbf{A}_{2g}$ or $\mathbf{A}_{2u})$, $\mathbf{A}_{1g}+\mathbf{E}_u$, $\mathbf{A}_{1u}+\mathbf{E}_g$, $\mathbf{A}_{2g}+\mathbf{E}_u$, $\mathbf{A}_{2u}+\mathbf{E}_g$.
$\mathbf{D}_{3h}$	$(\mathbf{A}_1'$ or $\mathbf{A}_1'')+(\mathbf{A}_2'$ or $\mathbf{A}_2'')$

[10] Slight modification of the XY_3 coordinate may be necessary to eliminate over-all rotation as in forming τ_s of Fig. 2 from ω_x, ω_y of XY_3, or to avoid distortion as in forming ω_x, ω_y of X_2Y_6 in Fig. 2 from $\mathbf{T}_x$, $\mathbf{T}_y$ of XY_3. We wish to thank Dr. J. B. Howard for calling our attention to this.

[11] J. B. Howard and E. B. Wilson, Jr., J. Chem. Phys. **3**, 630 (1934).

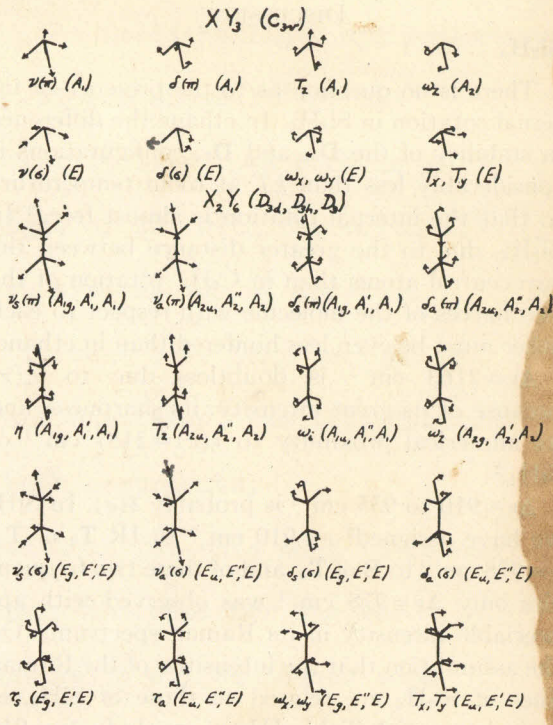

FIG. 2. Symmetry coordinates for X_2Y_6 from those for XY_3.

whereas the same operation changes the "out of phase" coordinates (those with subscript a) by 180° in phase. The equilibrium configuration for X_2Y_6 shown in Fig. 2 is that for symmetry $\mathbf{D}_{3d}$, but beneath each coordinate is noted the IR of the point groups $\mathbf{D}_{3d}$, $\mathbf{D}_{3h}$ and $\mathbf{D}_3$, respectively, to which the suitably drawn coordinate belongs when the $-XY_3$ radicals are combined to form molecules of these symmetries. These coordinates have been given designations for future reference.

In the following discussion we shall refer to these coordinates as if they were normal coordinates. The symmetry coordinates of $\mathbf{AB}_3$ have been chosen so that each one involves primarily a bending or a stretching of the bonds. For most $\mathbf{AB}_3$ molecules the large difference in the frequencies of the two vibrations belonging to either $\mathbf{A}_1$ or $\mathbf{E}$ of $\mathbf{C}_{3v}$ show that the normal coordinates are probably very similar to these symmetry coordinates. The same is probably true of the coordinates shown for $\mathbf{A}_2\mathbf{B}_6$. This would be expected to be true, especially for the degenerate modes, in case of free internal rotation.

Discussion

Si_2H_6

There is no question as to the presence of internal rotation in Si_2H_6. In ethane the difference in stability of the $\mathbf{D}_{3h}$ and $\mathbf{D}_{3d}$ configurations is considerably less than kT at room temperature so that the internal rotation is almost free.[12] In Si_2H_6, due to the greater distance between the two central atoms than in C_2H_6, rotation of the two halves of the molecule with respect to each other must be even less hindered than in ethane.

$\Delta\nu = 2163$ cm^{-1} is doubtless due to $\nu_s(\pi)$ because of its great intensity, its sharpness, and its numerical proximity to $\nu(\pi) = 2187$ cm^{-1} of SiH_4.[2]

$\Delta\nu = 910$ to 955 cm^{-1} is probably $\delta(\sigma)$. In SiH_4 we have assigned[2] $\nu = 910$ cm^{-1} to IR $\mathbf{T}_2$ of $\mathbf{T}_d$, $\nu = 978$ cm^{-1} to $\mathbf{E}$ of $\mathbf{T}_d$, and of these two frequencies only $\Delta\nu = 978$ cm^{-1} was observed with appreciable intensity in its Raman spectrum. On the assumption that the intensities of the Raman lines of Si_2H_6 are related to those of SiH_4, in accordance with Table III we conclude $\Delta\nu = 910$ to 955 cm^{-1} of Si_2H_6 probably belongs to $\mathbf{E}$ of $\mathbf{D}_3$, hence is probably $\delta(\sigma)$ rather than $\delta(\pi)$.

$\Delta\nu = 434.5$ cm^{-1} is very likely η. The fundamental frequencies of SiH_4 indicate that all the fundamental frequencies of Si_2H_6 are in the neighborhood of either 1000 cm^{-1} or 2000 cm^{-1} except η, ω_i and τ. ω_i is probably zero as nearly free internal rotation is present. η would be expected to be sharp, and perhaps of appreciable intensity because of its appearance in the Raman spectrum of C_2H_6 (g).[13] If it is assumed that 434.5 cm^{-1} is the frequency of vibration of two rigid $-SiH_3$ groups with respect to each other, a stretching force constant of 1.7×10^5 dynes/cm is found for the Si$-$Si bond.

Si_2Cl_6

In Si_2Cl_6 the situation as to internal rotation is not so clear. The electrostatic interaction due to assuming a positive charge of 4.5×10^{-10} e.s.u. on each Si atom and a negative charge of 1.5×10^{-10} e.s.u. on each Cl atom (corresponding to the high value of 3.0 Debyes for the dipole moment of the Si$-$Cl bond)[14] results in stabilizing the $\mathbf{D}_{3d}$ configuration by 475 cal./mole with respect to the $\mathbf{D}_{3h}$ configuration. The van der Waals attraction between the Cl atoms tends to stabilize the $\mathbf{D}_{3h}$ configuration by an amount of the order of 450 cal./mole.[15] Due to the mutual repulsion of the Cl atoms, there is a barrier of the order of 500 cal./mole between the two configurations.[16] Hence it seems probable that resistance to internal rotation at room temperature is probably of the order of $k\mathbf{T}$, the $\mathbf{D}_{3d}$ configuration being somewhat more stable than the $\mathbf{D}_{3h}$ one.

In accordance with Table IV we see that if Si_2Cl_6 possesses a rigid staggered ($\mathbf{D}_{3d}$) structure, six distinct fundamental frequencies are permitted in the Raman spectrum, three of which would have a polarization ratio $\rho < (6/7)$. If Si_2Cl_6 possesses a rigid structure having a symmetry plane perpendicular to the threefold axis, nine distinct fundamental frequencies are permitted to be Raman active, and three of these would have $\rho < (6/7)$.[17] If free internal rotation occurs the symmetry of the molecule is only $\mathbf{D}_3$ most of the time. For a rigid $\mathbf{D}_3$ model Table IV shows that ten distinct fundamental frequencies are permitted to be Raman active. However, if free rotation is present, one of these, ω_i, is zero, and intuitively it seems very likely that under such conditions the corresponding "in phase" and "out of phase" vibrations not symmetric with respect to the threefold axis (the degenerate vibrations) would become indistinguishable, thus resulting in only six distinct fundamental frequencies permitted in the Raman spectrum.

[12] Eucken and Weigert, Zeits. f. physik. Chemie **B23**, 266 (1933); Eucken and Parts, *Göttingen Nachrichten* (1932), p. 274; Zeits. f. physik. Chemie **B18**, 61 (1932); Eyring, J. Am. Chem. Soc. **54**, 3191 (1932).

[13] Teller and Topley, J. Chem. Soc. 885 (1935).

[14] Distances used: Si$-$Cl = 2.00A, the $SiCl_4$ value. Si$-$Si = 2.34A the value recently found in Si_2H_6 by electron diffraction. (Dr. Brockway, private communication.) The C$-$Cl dipole moment is about 1.5 Debyes and the Si$-$Cl separation is about twice the C$-$Cl separation on Pauling's electronegativity scale (See J. Am. Chem. Soc. **54**, 3570 (1932)).

[15] See Slater and Kirkwood, Phys. Rev. **37**, 682 (1931).

[16] If for the repulsive potential between two bound Cl atoms, the expression $\phi(r) = be^{(2\gamma_0-\gamma)/\rho}$ is used, with $b = 10^{-12}$ erg, $\rho = 0.2091$A, and $\gamma_0 = 1.370$A, the calculated barrier is about 350 cal./mole. These values of b and ρ were used to give the best fit for neon (see Bleick and Mayer, J. Chem. Phys. **2**, 252 (1934)) and γ_0 was chosen by comparison with γ_0 for neon and for the alkali and halide ions (see Huggins and Mayer, J. Chem. Phys. **1**, 643 (1933)). The barrier (exclusive of Coulomb interaction) calculated if the Cl atoms are assumed to be chloride ions is about 2000 cal./mole. (See Huggings and Mayer, above.) The correct value is probably nearer that calculated for bound chlorine atoms.

[17] By rigid here is meant that resistance to internal rotation is sufficiently great so that only small vibrations about the equilibrium position may occur.

In addition to the selection rules, we have some knowledge of the fundamental frequencies of $HSiCl_3$[18] and of $BrSiCl_3$[19] to aid us in our analysis of the Si_2Cl_6 spectrum. In Table VI are shown the observed Raman frequency shifts for these compounds and the assignment of the frequencies. The assignment shown for the $HSiCl_3$ frequencies is that of Mecke.[20] The analysis of the $BrSiCl_3$ frequencies we have made by analogy to Mecke's analysis[20] of the $HSiCl_3$, HCX_3 and CH_3X frequencies (X = halogen). The designations ν and δ refer to vibrations roughly approximated by the symmetry coordinates shown in Fig. 2 for XY_3 where X now becomes a rigid H−Si (or Br−Si) group, and $\eta(\pi)$ and $\eta(\sigma)$ refer, respectively, to vibrations in which the motion is essentially a stretching or a bending with respect to the $-SiCl_3$ group of the H−Si (or Br−Si) bond. Calculation of $\eta(\pi)$ for $BrSiCl_3$, assuming it to involve only a vibration of the Br atom relative to a rigid $-SiCl_3$ group and assuming the stretching force constant of the Si−Br bond to be unchanged from its value in $SiBr_4$, yields 314 cm^{-1}.

Considering both $BrSiCl_3$ and Si_2Cl_6 as a $-SiCl_3$ group with a rather large mass attached along the threefold axis, one would expect the $\nu(\pi)$ and $\delta(\pi)$ vibrations in one to be of approximately the same frequency as in the other. Without concluding as to the symmetry of Si_2Cl_6, this prediction coupled with the selection rules and the values of ρ for these lines lead us to assign 354 $cm^{-1} = \nu(\pi)$ and either 124 or 132 $cm^{-1} = \delta(\pi)$ in Si_2Cl_6.

Since the mass of the H atom is so small relative to that of Si or Cl, the frequencies of $HSiCl_3$ (omitting $\eta(\pi)$ and $\eta(\sigma)$)[21] are very nearly those of a free $-SiCl_3$ group. If nearly free internal rotation is present in Si_2Cl_6, the perpendicular vibrations $\nu(\sigma)$ and $\delta(\sigma)$ would be expected to be of nearly the same frequency as those of a free $-SiCl_3$ group, since then the net instantaneous momentum in any direction perpendicular to the threefold axis would be essentially zero for each half of the molecule. This condition need not obtain for a rigid[17] configuration. The appreciable intensity, the polarization ratio of 6/7, and the numerical value of 590 cm^{-1} in Si_2Cl_6 indicate that it is $\nu(\sigma)$. This proximity to the value of $\nu(\sigma) = 587$ cm^{-1} in $HSiCl_3$ favors the conclusion that there is nearly free internal rotation in Si_2Cl_6. The appreciable intensity and ρ value of 212 cm^{-1} lead to its assignment as $\delta(\sigma)$. This is slightly higher than $\delta(\sigma)$ in either $HSiCl_3$ (179 cm^{-1}) or $BrSiCl_3$ (183 cm^{-1}).

We are unable to make definite assignments of more than these four lines as fundamental frequencies of Si_2Cl_6. The relation of these assignments to the analyses of the frequencies of $HSiCl_3$, $BrSiCl_3$ and $SiCl_4$ from the viewpoint of Table III is shown in Table VII.

Several of the weaker lines observed may be assigned as combinations or overtones:

421 cm^{-1}: The first overtone of 212 cm^{-1}.
487 cm^{-1}: Combination 132 cm^{-1}+354 cm^{-1}.
565 cm^{-1}: Combination 212 cm^{-1}+354 cm^{-1}.
706 cm^{-1}: First overtone of 354 cm^{-1}.

The remaining weak lines, $\Delta\nu = 377$, 387 and 460 cm^{-1}, are also probably due to combinations or overtones. Numerically they agree with 124, 132 and 212 cm^{-1}, respectively, combining with a frequency of about 252 cm^{-1}. As fundamentals we can see no feasible assignment for them.

The component of the 124, 132 cm^{-1} doublet which is not $\delta(\pi)$ may well be τ with a polarization ratio of 6/7. The observed $\rho = 0.72$ is an over-all value for both lines.

Two possibilities suggest themselves for 179 cm^{-1}: (1) It may be η; (2) If the correct configuration is a rigid[17] one, it may be $\delta_a(\sigma)$, its numerical value being practically the same as $\delta(\sigma)$ in $HSiCl_3$ and $BrSiCl_3$. If η is assumed to be the vibration of two rigid $-SiCl_3$ groups with respect to each other, and if the Si−Si bond stretching

TABLE VI. *Assignment of the fundamental vibration frequencies of $HSiCl_3$ and of $BrSiCl_3$.*

$HSiCl_3$	IR	DESIGNATION	$BrSiCl_3$
489 (6.6)	A_1	$\nu(\pi)$	362 (V. STR.)
249 (2.6)	A_1	$\delta(\pi)$	123
2256 (8.3)	A_1	$\eta(\pi)$	325
587 (1)	E	$\nu(\sigma)$	410
179 (4)	E	$\delta(\sigma)$	183 (STR.)
797 (1)	E	$\eta(\sigma)$	201

[18] de Hemptinne and Peeters, Bull. Sci. Acad. Roy. Belg. **17**, 1107 (1931); Urey and Bradley, Phys. Rev. **37**, 843 (1931).
[19] de Hemptinne, Wouters and Fayt, Bull. Sci. Acad. Roy. Belg. **19**, 318 (1933).
[20] *Handbuch und Jahrbuch der Chem. Phys.* (Leipzig, 1934), Band 9, Teil II, p. 390.
[21] This is equivalent to calling the symmetry coordinates described above for $\eta(\pi)$ and $\eta(\sigma)$ normal coordinates.

TABLE VII. *Correlation of fundamental frequencies of $SiCl_4$, $HSiCl_3$, $BrSiCl_3$ and Si_2Cl_6.*

$SiCl_4$ (T_d)	$HSiCl_3$ (C_{3v})	$BrSiCl_3$	Si_2Cl_6	(D_3, D_{3d})(?)
A 425 (10)	489 (7)	362 (v. str.)	354 (10)	
	250 (3) A_1	123	124 (8)	A_1, A_{1g}
			or	
608 (2)	2258 (8)	325	132 (5)	
T_2 220 (5)				
	799 (1)	201		
E 150 (5)	587 (1) E	410	590 (3)	E, E_g
	179 (4)	183 (str.)	212 (4)	

force constant is that calculated above from Si_2H_6, its frequency should be 201 cm^{-1}. (A similar calculation using C_2H_6[13] and C_2Cl_6[22] data predicts a frequency of 354 cm^{-1} for η of C_2Cl_6, and a line belonging to the completely symmetric IR is observed at 342 cm^{-1}.) Since the frequency corresponding to the η vibration in C_2H_6, Si_2H_6 and C_2Cl_6 in each case appears with appreciable intensity in its Raman spectrum, we should expect it to appear also in Si_2Cl_6. Therefore it seems to us more likely that 179 cm^{-1} is η rather than $\delta_a(\sigma)$.

The observed line at $\Delta\nu = 625$ cm^{-1} appears with considerable intensity, yet it does not seem possible to us that it is due to a fundamental frequency. Its polarization ratio shows that it is not due to a degenerate fundamental frequency. Reference to Table IV shows that only $\nu_s(\pi)$, $\delta_s(\pi)$, η, and ω_i are permitted to be Raman active among the nondegenerate fundamentals in any of the models considered. Of these only $\nu_s(\pi)$ would be expected to be of relatively high frequency, but 354 cm^{-1} is definitely assigned as $\nu_s(\pi)$. $\Delta\nu = 625$ cm^{-1} must therefore be due to a combination or overtone. Its intensity then indicates that it probably corresponds to a level in accidental degeneracy with 590 cm^{-1}. Since 590 cm^{-1} shows a ρ value of 6/7 and 625 cm^{-1} a ρ value of <0.5, and since interaction between two levels may occur only if their wave functions belong to representations including the same IR, then the wave function corresponding to 625 cm^{-1} must belong to a representation including both $\mathbf{A}_1$ and $\mathbf{E}$ of the appropriate point group. Of the first overtones or one-one combinations for each of the symmetries $\mathbf{D}_3$, $\mathbf{D}_{3d}$ and $\mathbf{D}_{3h}$ only an overtone of a degenerate fundamental or a combination of two degenerate fundamentals belonging to the same IR satisfy this requirement.[23] If this interpretation is correct[24] either $2\delta(\sigma)$, 2τ or $\delta(\sigma)+\tau$ should be approximately 608 cm^{-1}, although this is not the case for the present proposed assignment. It is interesting to note that combination of 354 cm^{-1} with the hypothetical 252 cm^{-1} frequency gives a level at approximately 608 cm^{-1}, but this level would not satisfy the requirements just mentioned.

TABLE VIII. *Assignment of the Raman frequencies of Si_2Cl_6, assuming internal rotation.*[25]

$\Delta\nu$ cm^{-1}	Intensity	Assignment (See Fig. 2)
	Fundamentals	
354	10	$\nu_s(\pi)$
132 (or 124)	5 (or 8)	$\delta_s(\pi)$
179	0.4	η (?)
590	3	$\nu(\sigma)$
212	4	$\delta(\sigma)$
124 (or 132)	8 (or 5)	τ (?)
	Combinations and overtones	
421	$<<<1$	$2\delta(\sigma)$
487	$<<<1$	$\delta_s(\pi)+\nu_s(\pi)$
565	$<<1$	$\delta(\sigma)+\nu_s(\pi)$
706	$<<<1$	$2\nu_s(\pi)$
377	$<<1$	124 cm^{-1}+252 cm^{-1} (?)
387	$<<1$	132 cm^{-1}+252 cm^{-1} (?)
460	$<<<1$	$\delta(\sigma)$+252 cm^{-1} (?)
625	2	$\nu_s(\pi)$+252 cm^{-1} or (?) in accidental deg. with $\nu(\sigma)$ (?)

The above analysis does not permit a definite answer to the question of internal rotation in Si_2Cl_6 at room temperature, but affords some evidence for its existence. In Table VIII is shown a tentative assignment of the observed lines under the assumption that free rotation does exist.[25]

In conclusion we wish to thank Professor E. B. Wilson, Jr. and Dr. J. B. Howard for valuable criticism and discussion.

Note added in proof. Very recently Kemp and Pitzer (J. Chem. Phys. **4**, 749 (1936)) have presented evidence for the existence of a potential barrier of about 3150 cal./mole between the $\mathbf{D}_{3d}$ and $\mathbf{D}_{3h}$ configurations in ethane. Since the Si—Si distance (2.34A) in Si_2H_6 and Si_2Cl_6 is considerably greater than the C—C distance (1.52A) in ethane, their conclusions would not appear to exclude the possibility of internal rotation in Si_2H_6 and Si_2Cl_6.

[22] Heidenreich, Zeits. f. Physik **97**, 277 (1935).

[23] See Tisza, Zeits. f. Physik **82**, 48 (1933).

[24] In this case the numerical agreement between 587 cm^{-1} of $HSiCl_3$ and 590 cm^{-1} of Si_2Cl_6 loses some of its significance as evidence for free rotation.

[25] If instead a rigid (reference 17) $\mathbf{D}_{3d}$, or even $\mathbf{D}_{3h}$, structure exists, subscripts s on the degenerate frequency designations in Table VIII would be the only change necessary for the appropriate new tentative assignments.

KINETICS OF OXIDIZED SILVER SOLUTIONS

Note.

The following work was done with Mr. Alexander Kossiakoff under the direction of Professor Noyes during the summer of 1934. Unfortunately it was necessarily terminated before all the experiments contemplated could be performed. Some of the results have already been mentioned in published work[1] and in Dr. Coryell's thesis[3]. It should be mentioned that Coryell's work on the kinetics of oxidized silver solutions was done subsequent to this work. We are greatly indebted to Dr. Coryell for his assistance in the analysis of this data, and to Professor Swift for his constant advice during the pursuit of this work.

INTRODUCTION

Earlier work in this laboratory on the oxidation of silver nitrate solutions by ozone and on the rate of decomposition of these oxidized solutions is summarized in a recent article[1]. However the accuracy of these earlier experiments did not allow very quantitative treatment of the kinetics, partly due to the presence of unsuspected errors in the method of analysis. The objects of the present investigation were to make accurate measurements of the rate of oxidation by ozone of nitric acid solutions of silver nitrate, of the rate of decomposition of these argentic solutions, and of the steady state reached between these two rates, and to interpret these data.

The presentation of results is divided into the following consecutive sections: Method of Analysis, Experimental Technique, Treatment of Data, Reduction Rate, Oxidation Rate, Steady State, Summary.

METHOD OF ANALYSIS

Two separate results served to eliminate the method of analysis used in the earlier work:

1) The use of ferrous sulphate was precluded because experiments showed that a) 3n HNO_3 exerts appreciable oxidizing effect on ferrous sulphate solution in two to three minutes in the cold, b) 2n HNO_3 gave unreliable results with regard to consistency of titers of

ferrous sulphate solution by permanganate, and c) the titration of ferrous sulphate solution by permanganate in 1 n HNO_3 solution was very slow even when hot and the end point was not sharp.

2) The concentration of ozone during an oxidation run was not, as formerly assumed, that in an ozone saturated solution of nitric acid of the same strength as the solution to be analyzed. The rate of solution of ozone in nitric acid under the conditions of experiment was found to be quite slow and of the same order of magnitude as the rate of reduction of the ozone by the silver nitrate solution.

Considerable effort was spent in search of a rapid, accurate method of analysis for argentic silver in the presence of ozone. Several interesting facts were discovered before a suitable procedure was adopted. Some of these are briefly summarized here.

Action of Argentic Ion and of Ozone on Certain Reducing Agents.

These tests were made largely on samples of argentic nitrate or of ozone in either 2 n or 4 n HNO_3 solution and initially at 0°C.

The following reducing agents reduce both argentic ion and ozone completely in a short time as shown by immediate disappearance of the brown-black argentic color on adding an argentic solution or of the odor of ozone on adding an ozone sample to the reducing agent in a glass-stoppered flask:

$$Fe^{++},\ Fe(CN)_6^{=},\ \text{arsenite},\ Hg_2^{++},\ Mn^{++}.$$

In the case of Mn^{++}, the argentic solutions seem to oxidize it to permanganate but ozone seems to oxidize it to MnO_2 even with argentous

ion present. Thallous ion also reduces both, but the reduction of ozone is not complete within a few minutes (with shaking) unless a rather large excess of reagent is used. A ten-fold excess resulted in complete reduction of ozone in less than two minutes, and in much less time if argentic ion were also present.

The following reducing agents reduce argentic ion immediately, but within an hour with occasional shaking and with argentous ion present do not reduce ozone completely as shown by the persistence of the ozone odor:

$$HCOOH,\ C_2O_4^{=},\ H_2O_2,\ H_3PO_3,\ Cr^{+++}.$$

With Cr^{+++} after $2\frac{1}{2}$ hours chromate was scarcely detectable in the test with ozone.

Direct titration of argentic solutions using the disappearance of the argentic color as end point was found possible with a great number of reagents. In the absence of ozone comparison of such titrations with the thallium method of analysis[2] showed them to be quantitative within experimental error for all cases tested, namely $C_2O_4^{=}$, H_2O_2[4], and VO^{++}.

Comparison titration of two samples the same in argentic concentration but differing only in that one contained ozone whereas the other did not were carried out for a number of reagents. Of those listed above which do not completely reduce ozone in a short time, $C_2O_4^{=}$, H_2O_2, and HCOOH were tried and in each case showed partial reduction of ozone.

Chlorate ion is apparently very slowly, if at all, oxidized by argentic solutions.

From the above and other tests Cr^{+++}, Pb^{++}, and VO^{++} seemed to offer the most hope of reducing argentic ion without being affected by the presence of ozone. Pb^{++} is rapidly oxidized to PbO_2 by argentic ion if some PbO_2 is already present, but is only very slowly oxidized in the absence of PbO_2, the solid oxide apparently exerting a catalytic effect. Experiments with both Pb^{++} and Cr^{+++} showed that the presence of ozone had very little effect, but the results were not conclusive in showing precisely whether or not the effect were different from zero. VO^{++} was studied quite thoroughly. Argentic samples with ozone usually showed an oxidizing power toward VO^{++} some 5% higher than similar solutions free of ozone.

It was finally decided to use a reducing agent which completely and rapidly reduced both argentic ion and ozone, and to determine the ozone in a separate determination. For this purpose arsenite was chosen at Dr. Swift's suggestion.

Arsenite Method of Analysis.

The method of analysis finally adopted was to add the sample to an excess of neutral arsenite solution, precipitate the silver as chloride, neutralize with NaOH, and titrate the excess arsenite with iodine. If ozone was present, its concentration was found by deozonizing a second sample with a stream of air, absorbing the ozone from this stream by passage through buffered neutral KI solution, and titrating

with thiosulphate the iodine liberated on acidifying the iodide solution.

For testing the method the thallium method of analysis was used. This method was known[2] to be accurate in the absence of ozone, and further tests comparing it with the standard KI method for determining ozone showed that it also reduced one oxygen atom of ozone quantitatively. Similar tests with arsenite showed that it was quantitatively oxidized by ozone in the same manner. (See Table I). Comparison values of oxidizing power of the same argentic solution both with ozone present and absent by the thallous and arsenite methods of analysis are shown in Table II.

Further tests showed that 0.25 n arsenite was not oxidized appreciably in one hour by 5 n HNO_3 solution, but was almost completely oxidized by 7.5 n HNO_3 within that time. Also it was found that the presence of NO_2 in the nitric acid caused oxidation of the arsenite at an appreciable rate for acid concentrations less than 5 normal.

Table I

Reduction of Ozone by Arsenite Solution

	Milliequivalents O_3 per kg. of solution		
	A	B	C
KI Method	2.14, 2.16	2.73	2.44
Arsenite Method	2.17	2.77, 2.74	2.44

Table II

Comparison of Thallous and Arsenite Methods

	Oxidizing power in m.eq./kg.soln.	
	O_3 present	O_3 absent
Thallous Method	6.98, 6.99	2.48
Arsenite Method	6.98	2.50, 2.48

Materials.

The silver nitrate was purified by precipitation from concentrated nitric acid solution and carefully dried.

Ozone was prepared as described in Ref. 1. The current in the primary and the rate of flow of oxygen through the ozonizer were kept constant throughout oxidation runs so that the initial ozone content of the oxidizing stream was approximately 8%.

The other materials used were prepared by standard methods described elsewhere.

EXPERIMENTAL TECHNIQUE.

All runs were made at 0.00 ± 0.05°C using a water-alcohol bath in the thermostats described in Ref. 1. The reaction vessels are the same as used in the previous work. During oxidation runs the reaction vessel was preceded by a bottle of nitric acid of the same strength.

All samples were weighed and all concentrations calculated originally on a weight basis. Since the weighings could be performed

after the sample had been reduced this saved time and increased the accuracy of the determination.

Oxidation Rate and Steady State.

For each point of the rate curve two samples were taken. One yielded the sum of the argentic and ozone concentrations, the other the concentration of ozone in solution. The samples for ozone concentration were taken about in the middle of the time intervals between argentic samples.

Starting the run: A clean dry bottle was filled with HNO_3 (about 500 ml.) of known weight formality, the weight of HNO_3 recorded, and the bottle allowed to come to thermostat temperature and saturate with ozone under conditions to prevail during the run. Meanwhile the exact weight of dry $AgNO_3$ necessary to make a solution of the desired weight formality was weighed out in a small cylindrical glass container. To start the run this container was emptied into the mouth of the reaction bottle and then dropped in bodily. The flow of ozone was then interrupted at least twice during the first five minutes to allow the solution to become uniform in concentration both above and below the sintered glass filter plate of the reaction bottle.

Drawing samples: Samples of from 20 to 35 grams were used. For determining the sum of the argentic and ozone concentrations samples were drawn by suction so as to deliver beneath the surface of excess arsenite solution. The arrangement used is shown in Fig. 1.

FIGURE 1
Method of Drawing Samples.

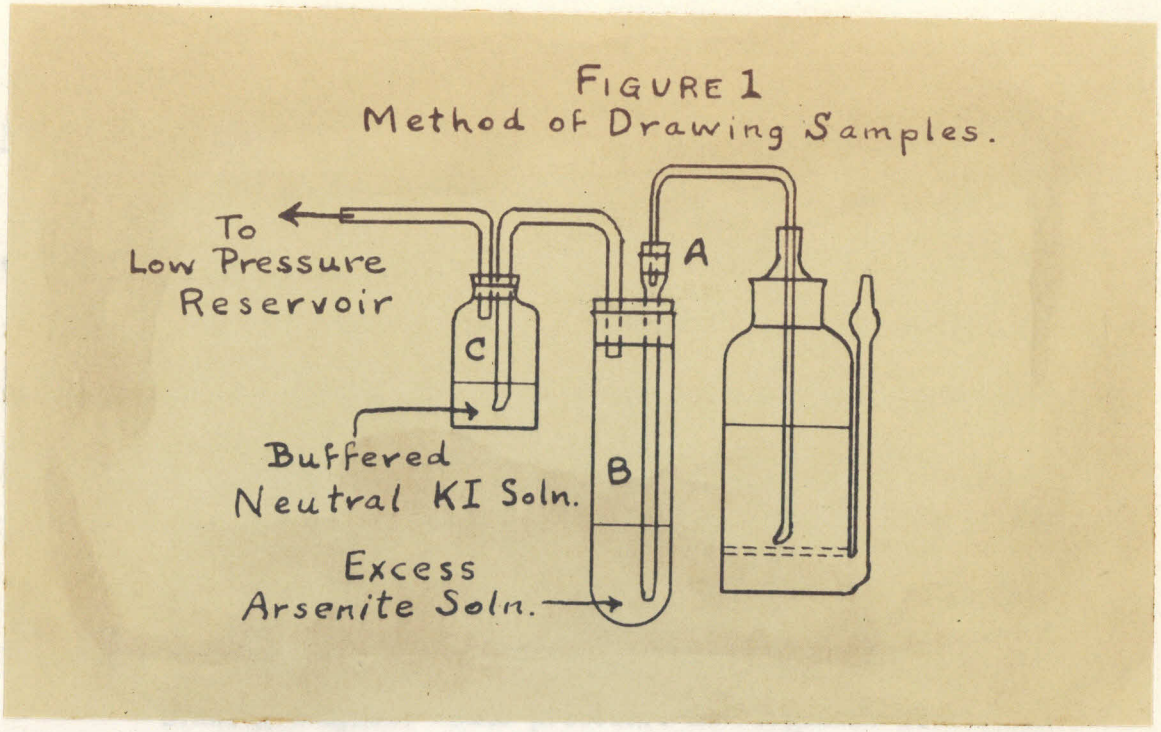

The rate at which the sample was drawn was regulated by stopcock. The flow was stopped by removing paraffined cork fitting at A and air drawn through for some thirty seconds to be certain any O_3 in gas phase is reduced and for mixing. The flow of ozone through the bottle was stopped just before drawing a sample and started immediately afterwards, a matter of some twenty seconds. A tube containing solid NaOH was placed in A on removing the cork fitting and delivery tube in order to prevent O_3 in the atmosphere from interfering. The delivery tube is dried and cooled before each sample.

For determining the ozone concentration in solution, B (Fig. 1) is empty and in place of C are used two large test tubes in series containing buffered neutral KI. The sample is drawn in the same way and air drawn through it for some ten minutes. There is no oxygen error with KI solution buffered to pH = 7.1

Reduction Rate.

Starting the run: The solution is made up by weight and allowed to be oxidized with constant conditions until the steady state is reached. After removing the steady state samples (oxidation technique) a swift stream of oxygen cooled by passage through a long copper coil in the thermostat is passed through the solution until passage of the stream through KI solution shows the absence of ozone. This requires some two to five minutes. A slow stream of oxygen is then maintained through the solution throughout the run.

Drawing samples: Same procedure as "argentic plus ozone" determinations of oxidation run.

For all reduction runs it was ascertained that no solid silver oxide(5) was present. This limited the total silver concentration which could be used.

TREATMENT OF DATA

The complicated nature of the kinetics involved made it highly important that the data be accurate. The internal consistency of each run is good. In Fig. 2 is shown the course of the oxidizing power due to argentic silver and to ozone in an oxidation and a reduction run. The runs in Fig. 2 show somewhat poorer consistency than most of the others. The appearance of Fig. 2 is characteristic of all oxidation and reduction runs.

FIGURE 2.

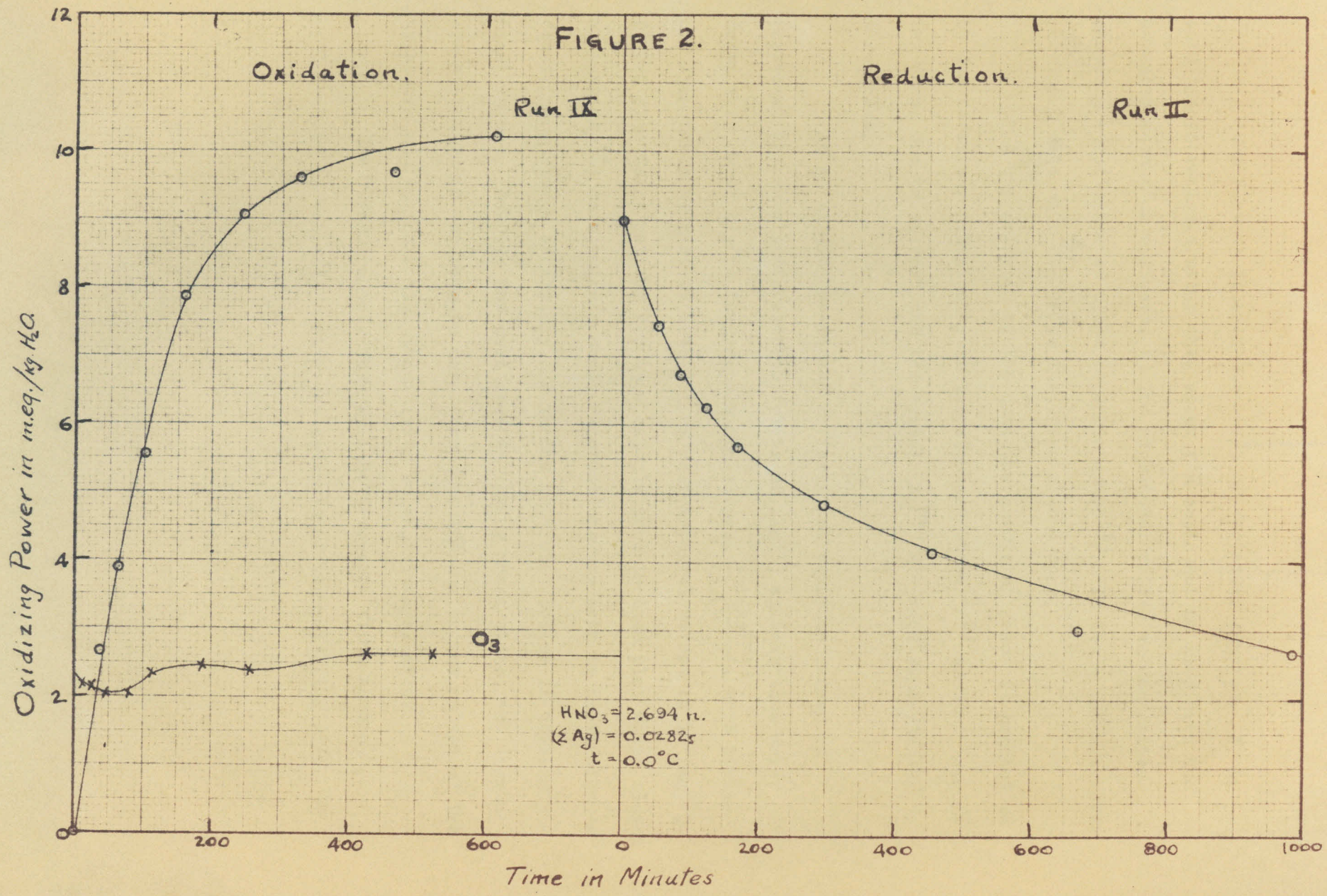

Two factors limited the range of variables studied. 1) An acid concentration greater than about 6 n could not be used with the arsenite method of analysis. 2) Too high total silver concentration caused precipitation of black argentic oxide[5]. In Table III are shown pertinent data with regard to the scope of the runs.

In the analysis of the data the oxidizing power is assumed to be due to silver principally in the divalent state[2,3] so that "oxidizing power due to silver" and the symbol (Ag^{++}) are used synonymously throughout.

As no simple one-termed differential equation seemed to represent the data satisfactorily plots of (Ag^{++}) against time were drawn very carefully on large scale and slopes, $\frac{-\Delta(Ag^{++})}{\Delta t}$, were picked off from these at various integral or half-integral values of $10^3(Ag^{++})$. It was also found helpful for some calculations to then plot these slopes against (Ag^{++}) to eliminate small fluctuations due both to difficulty in determining slopes accurately and to the use of a spline in drawing the first curves. Despite the care used in making these plots, the slopes are probably not accurate to more than 5 to 10% due to the nature of the treatment and to their high sensitivity to experimental error.

The reduction rate data will be discussed first as they will be used in connection with the analysis of the oxidation data.

Table III

Oxidation Runs

(All concentrations expressed in volume normal at 0°C.)

Run No.	(HNO_3)	(ΣAg)	10^3Final(Ag^{++})	10^3Final(O_3)	No. of points
VII	1.895	0.0284	8.09	2.28	5
VIII	1.895	0.0284	7.52	2.21	5
IX	2.692	0.0282	9.60	2.59	7
X	2.692	0.0564	13.42	2.16	8
XI	3.379	0.0272	9.11	2.16	7

Reduction Runs

Run No.	(HNO_3)	(ΣAg)	10^3Initial(Ag^{++})	10^3Final(Ag^{++})	No. of points
I	1.895	0.0284	6.90	2.20	10
II	2.692	0.0282	8.46	2.51	9
III	2.692	0.0564	12.08	4.45	11
IV	3.379	0.01958	8.07	3.47	11
V	3.379	0.0544	13.30	4.19	20
VI	3.379	0.0906	17.12	4.00	20

REDUCTION RATE

The earlier work[1] showed that at least under certain conditions the decomposition rate of the argentic solutions was apparently second order with respect to the argentic concentration and was

strongly dependent on the acidity. When $1/(Ag^{++})$ is plotted against time using our more accurate data it is clear that the rate is bi-molecular only in the final stages of the decomposition. (See Fig. 3a.) The shape of the curve shown in Fig. 3a is characteristic for all reduction runs, the curvature being greater for higher acidity and higher total silver concentration, (ΣAg).

Argentous Dependence, Acid Dependence, and Equilibrium between Valence States.

One of the first things noticed in treating the present data was that the slope approached in the last stages of the decomposition when $1/(Ag^{++})$ is plotted against the time (see Fig. 3a) was dependent on the argentous concentration. This dependence was found to be very probably inverse first power as shown in Table IV. This leads to the rate expression

$$-\frac{d(Ag^{++})}{dt} = k_2 \frac{(Ag^{++})^2}{(Ag^{+})} \qquad (1)$$

as representing the decomposition in the latter part of the runs.

This inverse dependence of rate on the argentous concentration as well as the high dependence on acidity early led us to believe that an equilibrium between tri-, bi-, and monovalent silver is probably involved. In view of the direct dependence of the oxidation rate on the argentous concentration (see Ref. 1 and below), it seemed that this equilibrium probably was represented by

FIGURE 3a.

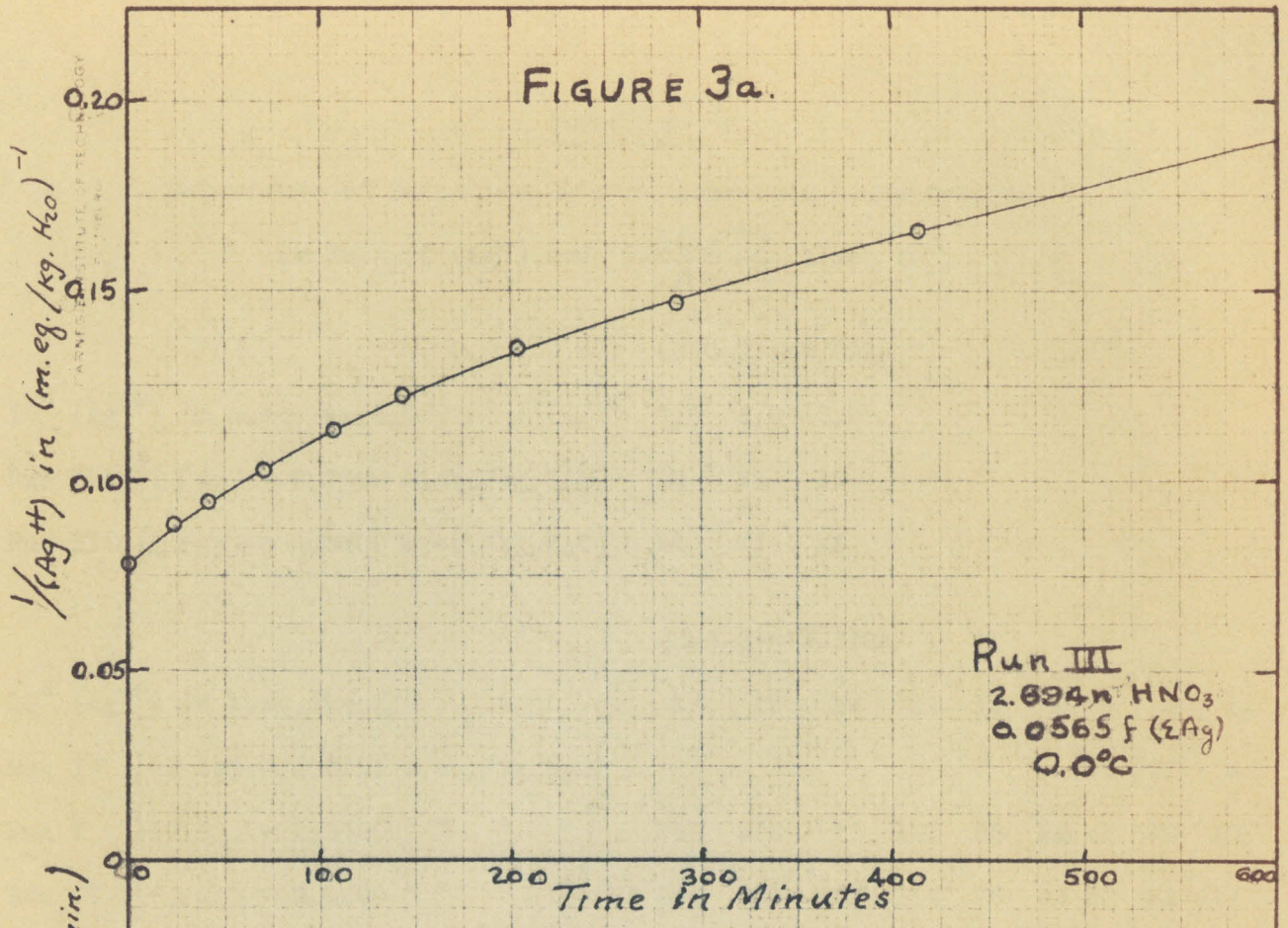

FIGURE 3b.

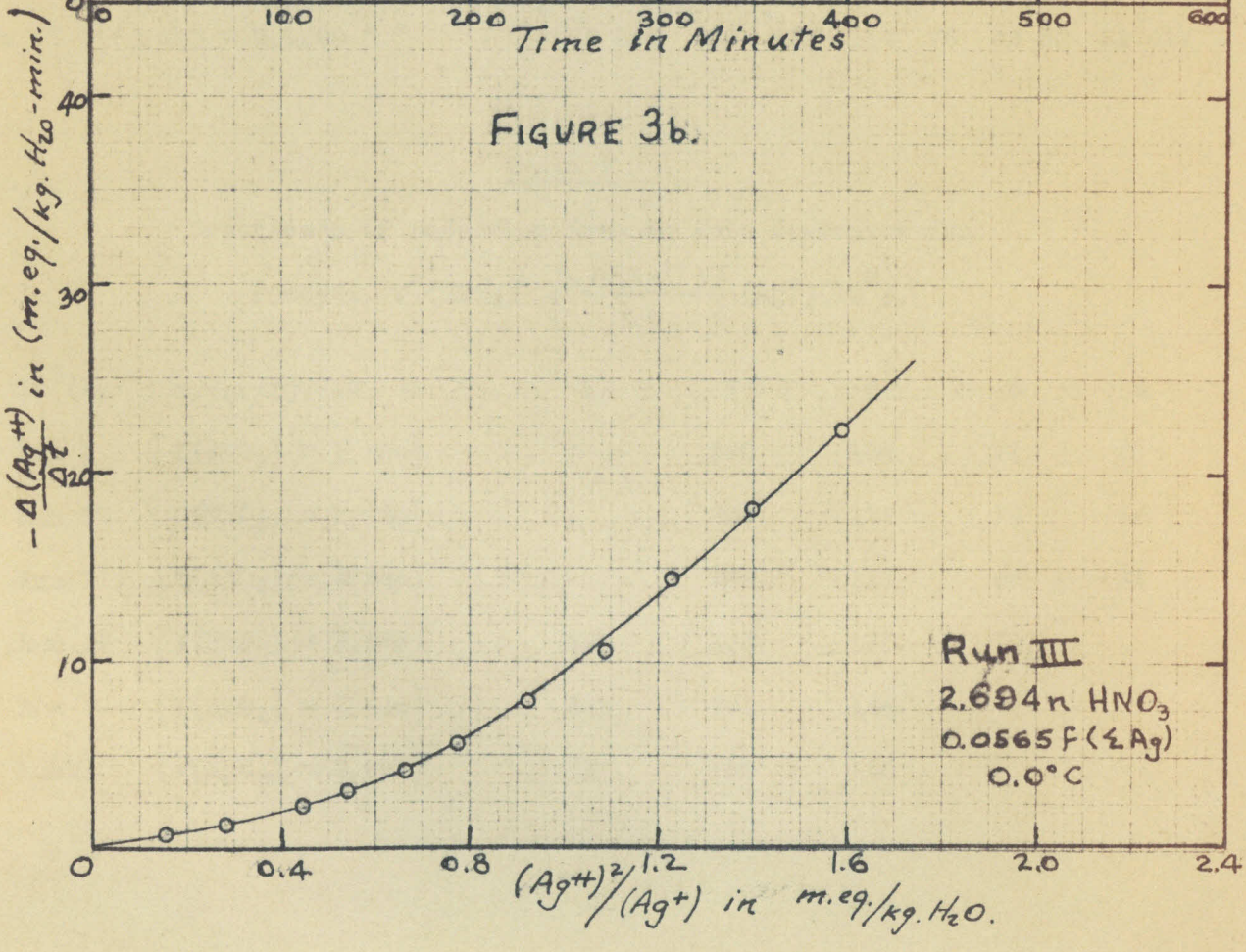

Table IV

Dependence of Reduction Rate on Argentous Concentration.

Product of (Ag^{+}) and $\frac{-\Delta(Ag^{++})}{\Delta t}$ times 10^{8}.

	$(HNO_3) = 2.692n$								
10^{3} (Ag^{++}) in m.eq./kg.H_2O	7.0	6.0	5.0						
Run II $\{(\Sigma Ag) = 0.0300$ m.eq./kg.$H_2O\}$	41	25	15						
Run III $\{(\Sigma Ag) = 0.0600$ m.eq./kg.$H_2O\}$	41	22	13						
	$(HNO_3) = 3.379n$								
10^{3} (Ag^{++}) in m.eq./kg.H_2O	14	13	12	11	10	9	8	7	6
Run IV $\{(\Sigma Ag) = 0.0215$ m.eq./kg.$H_2O\}$							34	23	14
Run V $\{(\Sigma Ag) = 0.0600$ " " " "$\}$	298	235	177	132	88	61	42	26	16
Run VI $\{(\Sigma Ag) = 0.1000$ " " " "$\}$	268	209	157	114	78	48	30	21	17

Table V

Dependence of Reduction Rate on Acid Concentration

Product $\gamma^{2}(HNO_3)^{2}\left[\frac{-\Delta(Ag^{++})}{\Delta t}\right](Ag^{+})(10^{8})$.

$10^{3}(Ag^{++})$ m.eq./kg.H_2O	8	7	6	5	4
Run I $\{\gamma(HNO_3) = 1.48n\}$		260	104	52	28
Run II $\{\gamma(HNO_3) = 2.25n\}$		209	127	76	45
Run III $\{\gamma(HNO_3) = 2.25n\}$		209	111	65	23
Run IV $\{\gamma(HNO_3) = 2.98n\}$	299	203	125	70	
Run V $\{\gamma(HNO_3) = 2.98n\}$	370	236	144		
RunVI $\{\gamma(HNO_3) = 2.98n\}$	271	190	150		

$$AgO^+ + Ag^+ + 2H^+ = 2Ag^{++} + H_2O \qquad (2)$$

Assuming then that the decomposition is first order with respect to (AgO^+), equation (2) leads to

$$-\frac{d(Ag^{++})}{dt} = (\text{constant})(AgO^+) = \frac{(\text{con})\,[Ag^{++}]^2\,[H_2O]}{[H^+]^2\,[Ag^+]} = \frac{k_2''(Ag^{++})^2}{\gamma^2_{H_2}(H^+)^2(Ag^+)} \qquad (3)$$

where the brackets are used for activities and parentheses for concentration. (k_2'' is a function of the activity of water and of the activity coefficients of Ag^+ and Ag^{++}).

Coryell[3] more recently has shown that in 9 n HNO_3 solution at 25° equ. (1) is quite well obeyed over most of the run and that the dependence of the reduction rate on acidity seems very roughly to be in accord with equ. (3). In Table V are shown values of $\gamma^2(HNO_3)^2(Ag^+)\ -\frac{\Delta(Ag^{++})}{\Delta t}$ for the same (Ag^{++}) in different runs. The rough constancy of these shows the overall rate dependence on acid strength at 0° is very approximately inverse square.

Equ. (1) however represents the decomposition rate only in the last stages of the reduction for runs at 0° as Fig. 3b clearly shows. This is true also at 25° at acid concentrations much below 9 n[3].

Fourth Order Argentic Dependence.

Plots of $-\frac{\Delta(Ag^{++})}{\Delta t}$ against many different functions of (Ag^{++}) and (Ag^{+}) for runs at the same acid strength were made by us and by Coryell with our data. No function could be found which satisfactorily represented the decomposition rate over the entire run corresponding to a one-term differential equation. Coryell[3], however, succeeded in showing, first with our data and later with his own, that if the differences between the actual curve found and the asymptote which it approached when $-\frac{\Delta(Ag^{++})}{\Delta t}$ was plotted against time be in turn plotted against $\frac{(Ag^{++})^4}{(Ag^{+})}$ the points determine roughly a straight line. This corresponds to the rate expression

$$-\frac{d(Ag^{++})}{dt} = k_2 \frac{(Ag^{++})^2}{(Ag^{+})} + k_4 \frac{(Ag^{++})^4}{(Ag^{+})} \qquad (4)$$

The relative values of k_2 and k_4 were found[3] to be such that at 25° and high acidity (9 n) the second order term was much larger than the fourth order one, but at lower acid concentrations at 25° and for all runs at 0° both terms made appreciable contributions to the rate.

Whether or not the fourth order term was dependent on $\frac{1}{(Ag^{+})}$ or on $\frac{1}{(Ag^{+})^2}$ was not clear from Coryell's treatment. If equ. (4) were true, however, by plotting $-\frac{\Delta(Ag^{++})}{\Delta t} \Big/ \frac{(Ag^{++})^2}{(Ag^{+})}$ against $(Ag^{++})^2$ a straight line should result, its slope being equal to k_4 and its intercept at $(Ag^{++})^2 = 0$ being k_2. If however

$$-\frac{d(Ag^{++})}{dt} = k_2' \frac{(Ag^{++})^2}{(Ag^+)} + k_4' \frac{(Ag^{++})^4}{(Ag^+)^3} \qquad (5)$$

be the correct equation, $-\frac{\Delta(Ag^{++})}{\Delta t} \Big/ \frac{(Ag^{++})^2}{(Ag^+)}$ plotted against $\frac{(Ag^{++})^2}{(Ag^+)}$ should give a straight line of slope k_4' and intercept k_2'. Plots of $-\frac{\Delta(Ag^{++})}{\Delta t} \Big/ \frac{(Ag^{++})^2}{(Ag^+)}$ against $(Ag^{++})^2$ and against $\frac{(Ag^{++})^2}{(Ag^+)}$ both determine approximately straight lines and are quite similar in appearance (since the argentous concentration does not change greatly in the course of a run), but the former show much better constancy in the values of k_4 than do the latter for values of k_4'. Figures 4 and 5 show the first type plot for all runs, and in Table VI are shown the values thus found for these constants. Values of $k_2 \gamma_{H^+}^2 (HNO_3)^2$ and $k_4 \gamma_{H^+}^2 (HNO_3)^2$ are also shown in Table VI illustrating their approximate inverse square dependence on the acid concentration.

Table VI

Comparison of Equ. (4) with Equ. (5).

Run	(HNO_3)	k_2 l/min.	k_4	k_2' l/min.	k_4'	$k_2 \gamma_{H^+}^2 (HNO_3)^2$	$k_4 \gamma_{H^+}^2 (HNO_3)^2$
I	1.895	0.0044	268	0.0025	8.9	0.010	585
II	2.692	0.0037	106	0.0043	1.9	0.019	535
III	2.692	0.0023	95	0.0008	8.9	0.012	480
IV	3.379	0.0019	76	0.0023	0.68	0.017	626
V	3.379	0.0020	86	0.0017	3.8	0.018	765
VI	3.379	0.0022	71	0.0017	5.9	0.020	632

k_4 in l/(min.)(m.eq./l.)

k_4' in l/(min.)(m.eq./l.)

FIGURE 4.

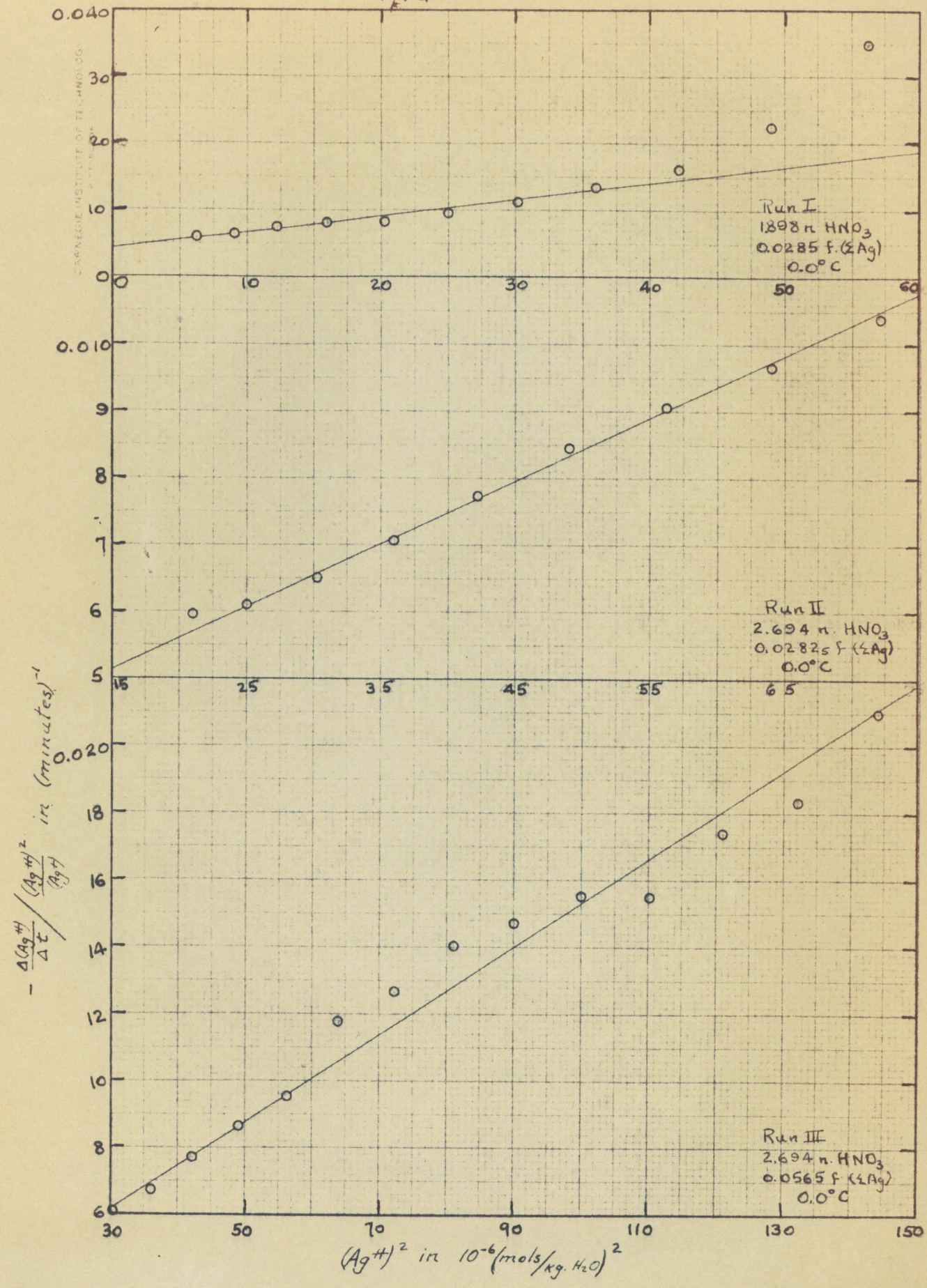
Run I
1.898 n. HNO_3
0.0285 f. (ΣAg)
0.0° C
Run II
2.694 n. HNO_3
0.02825 f. (ΣAg)
0.0° C
Run III
2.694 n. HNO_3
0.0565 f. (ΣAg)
0.0° C
$-\frac{\Delta(Ag^{\#})}{\Delta t}\Big/\frac{(Ag^{\#})^2}{Ag^{+}}$ in (minutes)$^{-1}$
$(Ag^{\#})^2$ in 10^{-6}(mols/kg. H_2O)^2

Mechanism.

The above analysis shows the observed decomposition rate is probably due to the simultaneous occurrence of two slow reactions, the one showing a second order and the other fourth order dependence on the oxidizing power.

The second order term of the reduction rate seems (see above and Ref. 1,3) to be very probably a result of the pseudounimolecular reaction

$$AgO^{+} + H_2O = H_2O_2 + Ag^{+} \qquad (6)$$

followed by the rapid decomposition of H_2O_2, probably[6,3] according to

$$H_2O_2 + 2Ag^{++} = O_2 + 2Ag^{+} + 2H^{+} \qquad (7)$$

The fourth order dependence, if it were represented by equ.(5), could be most simply represented by the bimolecular reaction

$$2AgO^{+} = 2Ag^{+} + O_2 \qquad (8)$$

combined with equ. (2). The rate equ. (4) is perhaps most simply (see also Ref. 3) represented by the pseudotrimolecular reaction

$$AgO^{+} + 2Ag^{++} + H_2O = 3Ag^{+} + O_2 + 2H^{+} \qquad (9)$$

combined with equ. (2). As discussed above our analysis shows that equ.(4) represents the data decidedly better than equ. (5). Also we have shown the overall acid dependence at 0° to be approximately an inverse square one. This is in accord with equ. (9), but equ. (8) indicates an inverse fourth power dependence on acidity for the fourth order reaction. Since the fourth order term of equ. (4) or equ. (5) is for conditions in our runs greater usually than the second order one,

we conclude that the observed decomposition rate is perhaps best explained by the mechanism involving the simultaneous occurrence of reactions (6) and (9).

OXIDATION RATE

In the earlier work[1] it was found that the initial oxidation rate was probably directly proportional to the ozone and argentous concentrations and independent of acidity. Our data confirm these results with regard to the argentous and acid concentrations. The percentage of ozone was practically the same in all of our runs.

In order to test this rate dependence over more than the initial stages of the oxidation it is necessary to take into account the reduction rate as well. Accordingly we write

$$\frac{d(Ag^{++})}{dt} = k_o(Ag^+)(O_3) - \text{reduction rate} \qquad (10)$$

where for the reduction rate we can calculate values using equ. (4), or can use the "experimental" values from plots of (Ag^{++}) against time for the reduction runs. In Table VII are shown values of k_o calculated by equ. (10) for various argentic concentrations in the course of a run, using the "experimental" values for the reduction rate. In Table VIII are shown the mean values of k_o so calculated for each run. These values show that equ. (10) does fit the data reasonably well.

The mechanism of the oxidation reaction is accordingly very probably[1]

$$Ag^+ + O_3 = AgO^+ \qquad (11)$$

followed by the rapid equilibrium (2).

Table VII

Values of k_o, Equ. (10), for a Single Run

$10^3(Ag^{++})$ in m.eq. per kg.H_2O	$10^6 \frac{\Delta(Ag^{++})}{\Delta t}$ Oxidation	$-10^6 \frac{\Delta(Ag^{++})}{\Delta t}$ Reduction	(O_s) m.mols/kg.H_2O	$10^3(Ag^+)$ m.eq./kg.H_2O	k_o $\frac{1}{(min)(mols/liter)}$
0 - 2	118		~1.00	59	2.12
7	91	8	0.84	53	2.36
8	83	14	0.85	52	2.31
9	83	21	0.87	51	2.46
10	63	30	0.90	50	2.19
11	45	41	0.95	49	2.19
11.5	38	48	0.99	48.5	1.89
12.0	31	57	1.02	48	1.91
12.4	25	68	1.03	47.6	1.97
				Mean	2.16
				Average deviation from mean	0.16

Table VIII

Oxidation Rate Constant k_o, Equ. (10)

Run	(HNO_3) mols/liter	(ΣAg) mols/liter	Mean k_o in $\frac{1}{(min.)(mols/liter)}$	Average Deviation from Mean k_o
VII	1.89	0.0284	1.94	0.24
VIII	1.89	0.0284	2.22	0.28
IX	2.69	0.0282	2.21	0.20
X	2.69	0.0564	2.16	0.16
XI	3.38	0.0272	2.27*	0.30
			Mean 2.16	

*Reduction rate calculated from Equ. (4).

STEADY STATE

The steady state reached on prolonged passage of ozone through a nitric acid solution of silver nitrate is presumably the point at which the reduction rate and the oxidation rate just balance. The above analysis of the oxidation and reduction rates shows that this should be true when

$$\frac{d(Ag^{++})}{dt} = 0 = k_0(Ag^{+})(O_3) - k_2 \frac{(Ag^{++})^2}{(Ag^{+})} - k_4 \frac{(Ag^{++})^4}{(Ag^{+})} \qquad (12)$$

provided no further complicating factors enter. In Table IX are shown the steady state data with the calculated oxidation and reduction rates using $k_0 = 2.16$ (liters)/(min)(mols) (See Table VIII.) and values of k_2 and k_4 shown in Table VI. Although the calculated forward and backward rates do differ appreciably in most cases, the conclusion seems justified that the steady state involves no new processes not already met with in the oxidation and reduction analyses. The discrepancies in the calculated rates at the steady state are probably due largely to the use of inaccurate values of the constants and partly to experimental error.

Table IX

Steady State Data

(HNO_3) mols/liter	$10^3(Ag^{++})^a$	$10^3(Ag^+)^a$	$10^3(O_3)^a$	10^6 Oxidn.^{b} Rate	10^6 Redn.^{b} Rate	Ratio Oxidn. Rate / Redn. Rate
1.865	8.54	21.4_6	2.41	52.7	74.5	0.71
	7.94	22.0_6	2.33	52.5	55.7	0.94
	8.03	21.9_7	2.09	47.8	56.2	0.85
	8.16	21.8_4	2.15	47.9	62.1	0.79
3.345	8.93	12.6_7	2.16	26.8	43.3	0.62
	8.83	12.7_7	2.30	28.8	41.3	0.70
	8.98	12.6_2	2.34	29.0	44.3	0.66
	8.83	12.7_7	2.38	29.9	41.3	0.73
	15.00	45.00	1.548	68.3	89.3	0.76
	15.08	44.92	1.530	62.4	91.4	0.68
	13.72	80.28	1.026	80.7	121.0	0.67
	19.85	80.15	1.149	90.3	124.3	0.73
2.672	9.59	20.41	2.32	48.0	55.7	0.86
	9.64	20.36	2.26	46.7	56.6	0.83
	10.20	19.80	2.65	53.3	70.8	0.75
	14.35	45.65	2.23	103.4	88.8	1.16
	14.27	45.73	2.30	107.0	86.7	1.23
	12.91	47.09	1.93	92.5	57.7	1.60
	13.29	46.71	1.86_6	88.5	65.0	1.36
	13.56	46.44	1.86_6	88.0	70.7	1.25
					Mean	0.90

[a] in equ./kg. H_2O [b] in equ./(kg.H_2O)(min.).

SUMMARY

The behavior of a number of reducing agents toward nitric acid solutions of argentic silver and of ozone has been observed. Argentic solutions may be reduced quantitatively by titration with any of a number of reducing agents using the disappearance of the argentic color as end-point.

The rate of oxidation by ozone of nitric acid solutions of silver nitrate and the rate of decomposition of these oxidized solutions has been studied using suitable technique and method of analysis. The reduction rate is found to fit the differential equation

$$-\frac{d(Ag^{++})}{dt} = k_2 \frac{(Ag^{++})^2}{(Ag^{+})} + k_4 \frac{(Ag^{++})^4}{(Ag^{+})} \qquad (4)$$

indicating simultaneous occurrence of two slow reactions. (The oxidized silver is assumed to be principally in the divalent state[2,3].) The oxidation rate is found to fit the equation

$$\frac{d(Ag^{++})}{dt} = k_o(Ag^{+})(O_3) - \text{reduction rate} \qquad (10)$$

The steady state reached on prolonged oxidation by ozone of nitric acid solutions of silver nitrate is shown to correspond approximately to the point where $\frac{d(Ag^{++})}{dt} = 0$ in equ.(10) and reduction rate is given by equ. (4).

Equilibrium between three valence states of silver is postulated, probably according to the reaction

$$AgO^{+} + Ag^{+} + 2H^{+} = 2Ag^{++} + H_2O \qquad (2)$$

The oxidation mechanism[1] is probably

$$Ag^+ + O_3 = AgO^+ + O_2$$

and the second order reduction reaction is probably

$$AgO^+ + H_2O = Ag^+ + H_2O_2$$

with equ. (2). The fourth order reduction reaction may be[3]

$$H_2O + 2Ag^{++} + AgO^+ = 3Ag^+ + O_2 + 2H^+ \qquad (9)$$

References

(1) Noyes, Hoard, and Pitzer, J.A.C.S., 57, 1221 (1935).

(2) Noyes, Pitzer, and Dunn, J.A.C.S., 57, 1229 (1935).

(3) Coryell, Thesis, Calif. Inst. Tech., 1935.

(4) We are thankful to Mr. Robert Heitz for testing the H_2O_2 titration.

(5) On prolonged oxidation by ozone of silver nitrate solutions in nitric acid a black, emery-like solid may separate out if the total silver concentration is sufficiently high. This is probably argentic oxide. Two determinations of a sample of this solid showed oxidizing equiv. of 0.99 and 1.05 per g. atom of silver, indicating divalent silver.

(6) Noyes and Kossiakoff, J.A.C.S., 57, 1238 (1935).